Developmental Cell
Article

Oskar Is Targeted for Degradation by the Sequential Action of Par-1, GSK-3, and the SCF^{-Slimb} Ubiquitin Ligase

Eurico Morais-de-Sá,[1,2,3,4] Antonio Vega-Rioja,[1,2,3,5] Vítor Trovisco,[1,2] and Daniel St Johnston[1,2,*]
[1]The Gurdon Institute
[2]Department of Genetics
University of Cambridge, Tennis Court Road, Cambridge CB2 1QN, UK
[3]These authors contributed equally to this work
[4]Present address: Instituto de Biologia Molecular e Celular (IBMC), Porto 4150-180, Portugal
[5]Present address: Servicio Regional de Inmunología y Alergia, Hospital Universitario Virgen Macarena, Seville 41009, Spain
*Correspondence: d.stjohnston@gurdon.cam.ac.uk
http://dx.doi.org/10.1016/j.devcel.2013.06.011
This is an open-access article distributed under the terms of the Creative Commons Attribution-NonCommercial-No Derivative Works License, which permits non-commercial use, distribution, and reproduction in any medium, provided the original author and source are credited.

SUMMARY

Translation of *oskar* messenger RNA (mRNA) is activated at the posterior of the *Drosophila* oocyte, producing Long Oskar, which anchors the RNA, and Short Oskar, which nucleates the pole plasm, containing the posterior and germline determinants. Here, we show that Oskar is phosphorylated by Par-1 and GSK-3/Shaggy to create a phosphodegron that recruits the SCF^{-Slimb} ubiquitin ligase, which targets Short Oskar for degradation. Phosphorylation site mutations cause Oskar overaccumulation, leading to an increase in pole cell number and embryonic patterning defects. Furthermore, the nonphosphorylatable mutant produces bicaudal embryos when *oskar* mRNA is mislocalized. Thus, the Par-1/GSK-3/Slimb pathway plays important roles in limiting the amount of pole plasm posteriorly and in degrading any mislocalized Oskar that results from leaky translational repression. These results reveal that Par-1 controls the timing of pole plasm assembly by promoting the localization of *oskar* mRNA but inhibiting the accumulation of Short Oskar protein.

INTRODUCTION

Asymmetric accumulation of proteins within single cells is critical to establish polarity, segregate cell fate determinants, and to specify the body axis of multicellular organisms. In *Drosophila*, Oskar (Osk) protein accumulates at the posterior of the oocyte to direct the formation of a specialized cytoplasm, the pole plasm, which determines posterior patterning and germ cell formation after fertilization (Breitwieser et al., 1996; Markussen et al., 1995; Vanzo and Ephrussi, 2002). The levels of Osk protein directly correlate with the number of germ cells and the embryonic pattern (Ephrussi and Lehmann, 1992; Smith et al., 1992). Furthermore, ectopic expression of Osk at the anterior induces a duplication of posterior structures and specification of anterior pole cells (Ephrussi and Lehmann, 1992; Smith et al., 1992). The localized accumulation of Osk is therefore strictly controlled at several levels, including the localized transport and translation of its messenger RNA (mRNA) and the anchoring of *osk* mRNA and protein at the posterior (for review, see Kugler and Lasko, 2009). There are two Osk protein isoforms produced by selective use of two alternative in-frame start codons in the Osk coding sequence. Long Osk is required to anchor *osk* mRNA and Short Osk protein to the posterior cortex but does not function as a determinant, whereas Short Osk initiates the assembly of the pole plasm (Breitwieser et al., 1996; Markussen et al., 1995; Vanzo and Ephrussi, 2002).

Par-1 kinase is a major regulator of cell polarity in multiple biological contexts (St Johnston and Ahringer, 2010). Par-1 localizes at the oocyte posterior and controls the formation of a polarized microtubule cytoskeleton by excluding microtubule minus ends from the oocyte posterior (Doerflinger et al., 2010; Shulman et al., 2000; Tomancak et al., 2000). This polarized microtubule network then directs the localization of *osk* mRNA to the posterior pole of the oocyte (Zimyanin et al., 2008). It has also been reported that Par-1 directly phosphorylates Osk protein to prevent its degradation (Riechmann et al., 2002). Although this work did not decipher the molecular mechanism involved in Osk destabilization, it suggests that the regulation of Osk protein stability might confer another layer of control over the level of this crucial posterior determinant.

Here, we show that Osk stability is regulated by Slimb (β-TRCP), an F-box protein that is the substrate recognition subunit of the SKP1/Cullin/F-box (SCF) protein E3 ubiquitin ligase complex that targets proteins for proteosomal-dependent degradation (Cardozo and Pagano, 2004). Slimb recognizes the doubly phosphorylated DpSGXXpS destruction motif (Degron) present in Armadillo/β-catenin and IκB (Maniatis, 1999). Sgg/GSK-3 kinase is required for Slimb-mediated degradation of Armadillo/β-catenin and Cubitus interruptus (Ikeda et al., 1998; Smelkinson and Kalderon, 2006). Importantly, Sgg/GSK-3 phosphorylation requires a priming phosphorylation by another

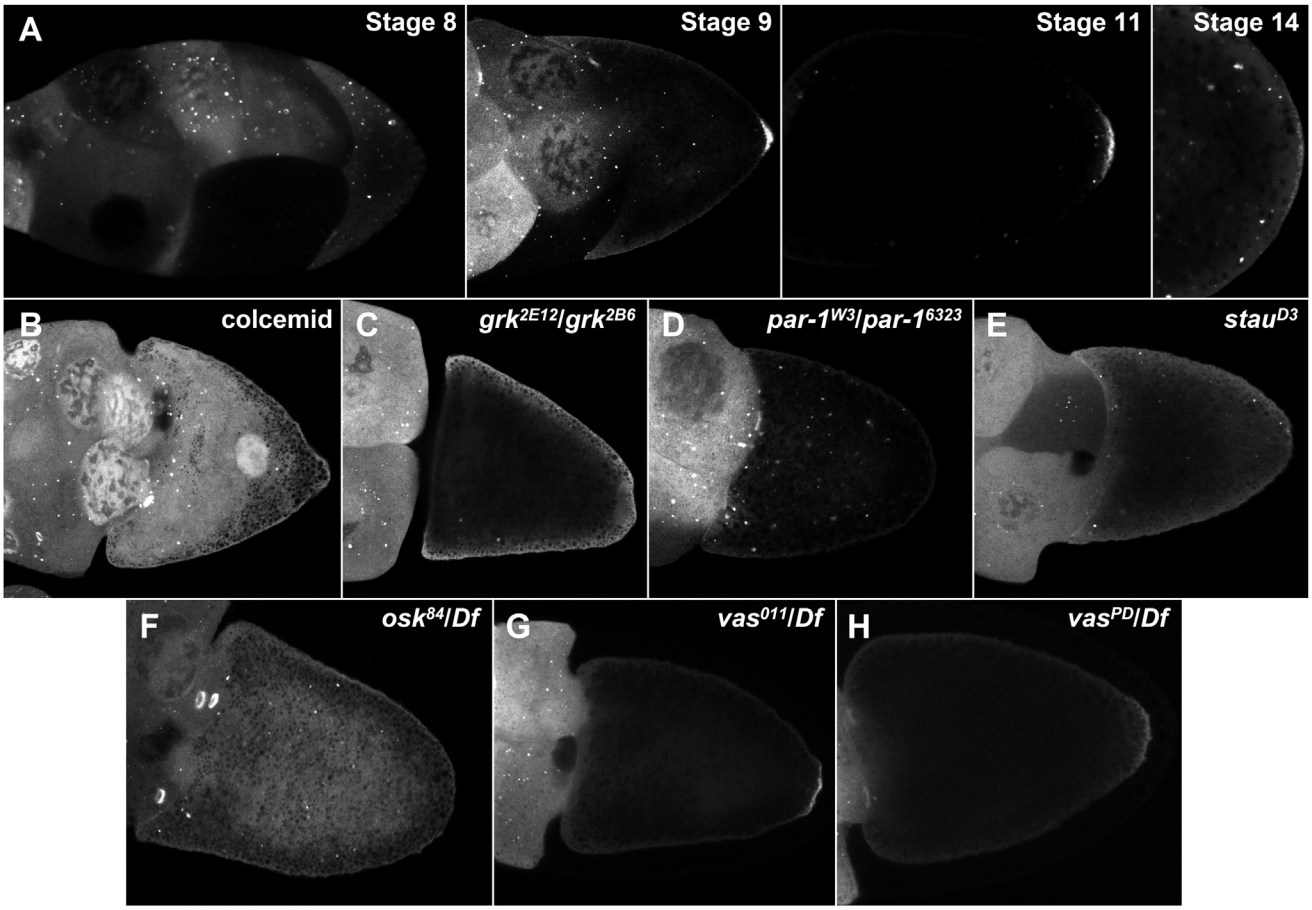

Figure 1. Slimb Accumulates at the Posterior of the Oocyte in an Osk-Dependent Manner

(A) GFP-Slimb localizes to the oocyte posterior from stage 9 onward, but this localization is reduced in mature oocytes.

(B) GFP-Slimb localization in an oocyte from a female treated with colcemid to depolymerize microtubules. Mislocalization of the oocyte nucleus confirms the efficiency of drug treatment.

(C–H) GFP-Slimb localization in mutants that disrupt oocyte polarity or pole plasm assembly: grk^{2E12}/grk^{2B6} (C), $par\text{-}1^{W3}/par\text{-}1^{6323}$ (D), $stau^{D3}$ (E), and $osk^{84}/Df(3R)p^{XT103}$ (F) abolish the posterior localization of Slimb, indicating that its posterior recruitment depends on the localization of Osk protein, whereas Slimb localizes at the posterior in $vas^{011}/Df(2L)A267$ (G) and $vas^{PD}/Df(2L)A267$ (H), which block the assembly of the pole plasm downstream of Osk. (A–H) UAS-GFP-Slimb was expressed in the germline using a *nanos-GAL4:VP16* driver.

kinase (Dajani et al., 2001; Fiol et al., 1987; Jia et al., 2002; Price and Kalderon, 2002). We show that Par-1 primes Osk for GSK-3 phosphorylation to form a phosphodegron, thereby targeting Osk for degradation, rather than stabilizing it as previously proposed.

RESULTS

Slimb Is Recruited to the Oocyte Posterior by Short Osk

We recently identified *slimb*, the ortholog of human β-TRCP, in a germline clone screen for mutants that disrupt the polarity of the oocyte (E.M. and D.StJ., unpublished data; Martin et al., 2003). During the course of this work, we discovered that Slimb protein accumulates at the oocyte posterior from stage 9 onward, i.e., after the oocyte has been polarized, suggesting an additional role during *Drosophila* oogenesis. We therefore investigated how Slimb is targeted to the posterior cortex using a GFP-tagged Slimb transgene that faithfully reproduces the localization of the endogenous protein. GFP-Slimb is first recruited to the posterior at stage 9 of oogenesis and remains there throughout most of mid/late oogenesis, but it largely disappears by stage 14 when the oocytes have matured (Figure 1A).

To determine how Slimb is recruited to the posterior, we analyzed its localization under various conditions that disrupt the polarization of the oocyte and the formation of the pole plasm. Treatment with the microtubule-depolymerizing drug, colcemid, blocks the posterior enrichment of Slimb, suggesting that this depends on a polarized microtubule cytoskeleton (Figure 1B). Consistent with this, Slimb is not localized in *gurken* and *par-1* mutants, which disrupt the polarity of the oocyte upstream of microtubule organization (González-Reyes and St Johnston, 1994; Roth et al., 1995; Shulman et al., 2000; Tomancak et al., 2000) (Figures 1C and 1D). A key function of the polarized microtubule network in the oocyte is to direct the transport of *osk* mRNA to the posterior cortex (Clark et al., 1994; Zimyanin et al., 2008). *osk* mRNA localization and anchoring at the

posterior require the RNA-binding protein, Staufen (Stau), which colocalizes with the mRNA at the posterior pole (Ephrussi et al., 1991; Kim-Ha et al., 1991; St Johnston et al., 1991). *stau* mutants also abolish Slimb localization, indicating that Slimb recruitment to the posterior is downstream of the localization of Stau and *osk* mRNA (Figure 1E).

We next asked whether Osk protein is required for Slimb localization using a nonsense allele, osk^{84}, in which *osk* mRNA localizes normally at stage 9, but produces no protein (Ephrussi et al., 1991; Kim-Ha et al., 1991; St Johnston et al., 1991). Slimb is not localized posteriorly in osk^{84}/Df oocytes, demonstrating that Slimb recruitment depends on Osk protein or a downstream component of the pole plasm (Figure 1F). To distinguish between these possibilities, we analyzed Slimb localization in a hypomorphic allele of *vasa*, vas^{011}, which lacks catalytic activity, preventing the subsequent steps of pole plasm assembly (Liang et al., 1994). GFP-Slimb still accumulates posteriorly in vas^{011} but shows a reduced localization in the stronger *vasa* mutant allele, vas^{PD} (Figures 1G and 1H). This latter allele abolishes the posterior localization of Vasa and reduces the amount of posterior Osk protein, because Vasa participates in a positive feedback loop to enhance Short Osk accumulation (Breitwieser et al., 1996; Markussen et al., 1995; Rongo et al., 1995). Thus, Slimb seems likely to be directly recruited to the posterior by Osk, because its localization does not depend on Vasa or any downstream steps in pole plasm assembly and correlates with the amount of localized Osk protein.

To determine whether the posterior recruitment of Slimb depends on the Long or Short isoform of Osk, we examined the localization of endogenous Slimb in *osk* RNA null oocytes expressing either an osk^{M1L} transgene that can only produce Short Osk or an osk^{M139L} transgene that produces only Long Osk (Markussen et al., 1995). Long Osk is necessary and sufficient for the anchoring of Short Osk and Stau protein at the posterior (Vanzo and Ephrussi, 2002). Consistent with this, when Short Osk is expressed alone, Stau and Osk protein spread away from the posterior cortex, and Slimb localizes in these detached particles (Figures 2A and 2B). By contrast, Slimb is absent from the posterior of oocytes expressing only Long Osk, despite the normal localization of Stau (Figure 2C). These results imply that the posterior recruitment of Slimb depends specifically on Short Osk. To confirm this hypothesis, we targeted either Long or Short Osk to the anterior of the oocyte using transgenes in which the *osk* 5′UTR and coding region are fused to *bcd* 3′UTR (Ephrussi and Lehmann, 1992; Tanaka and Nakamura, 2008). Expression of Short Osk (osk^{M1L}-*bcd3′UTR*), but not Long Osk (osk^{M139L}-*bcd3′UTR*), recruits GFP-Slimb to the anterior (Figures 2D and 2E). Furthermore, ectopic localization of Short Osk recruits Slimb during earlier stages to sites in which *bcd* mRNA is normally located (Figure 2F). Thus, Short Osk is necessary and sufficient for Slimb localization at either the anterior or posterior of the oocyte, suggesting that it recruits Slimb directly.

In order to better understand the mechanism of Slimb recruitment to the posterior of the oocyte, we produced transgenes expressing GFP-Slimb lacking the F-Box (Slimb-Δ-F-Box) or the WD40 repeats (Slimb-Δ-WD40). As the F-Box domain is required for Slimb's interaction with the rest of the SCF complex and the WD40 repeats bind to SCF^{Slimb} substrates, the localization of these truncated GFP-Slimb transgenes should indicate if Osk recruits Slimb directly because it is a substrate or indirectly by recruiting the rest of the SCF complex. GFP-Slimb-Δ-F-Box localizes to the posterior as efficiently as full-length Slimb, whereas GFP-Slimb-Δ-WD40 does not accumulate posteriorly (Figures 2G and 2H). Thus, Slimb localization at the posterior depends on its substrate interaction domain but is independent on its interaction with the rest of SCF complex.

To address if Slimb is a stable component of the pole plasm or continually turns over at the posterior, we performed fluorescence recovery after photobleaching (FRAP) experiments with GFP-Slimb-Δ-F-box (Figure S1 available online). The GFP-Slimb-Δ-F-box signal returns to around 60% of its prebleaching level in 10 min, which is comparable to other dynamically localized components within the oocyte, such as *grk* and *bcd* mRNAs (Jaramillo et al., 2008; Weil et al., 2006). Thus, Slimb is constantly recruited to the posterior, consistent with the hypothesis that it recognizes a substrate that is constantly produced at the posterior.

Slimb Regulates Excessive Osk Protein Levels via Protein Ubiquitylation

As the posterior localization of Slimb requires its substrate-interacting domain and Short Osk, Osk is a good candidate to be a substrate for polyubiquitylation by the SCF complex. We therefore analyzed Osk protein levels in ovary extracts from combinations of *slimb* hypomorphic mutants rescued to adulthood by larval expression of hs-Slimb (Figure 3A). Short Osk is strongly overexpressed in $slimb^{8}/slimb^{9H4\text{-}17}$ and $slimb^{8}/slimb^{1}$ mutant ovaries, and this is largely rescued by germline expression of GFP-Slimb. In contrast to Osk, the levels of Vasa do not change under any of these conditions. Thus, Slimb appears to specifically target Short Osk for degradation.

The observation that Osk levels are increased in *slimb* mutants raises the question of whether Slimb is involved in the spatial control of Osk accumulation or whether it simply acts to limit Osk levels. We therefore examined the distribution of Osk in *slimb* mutant oocytes, focusing on transheterozygous combinations of hypomorphic mutants that rarely disrupt oocyte polarity. The most frequent defect in these oocytes is the enlargement of the Osk, Stau, and Vasa staining at the posterior, coupled with a failure to form a tight posterior crescent (Figures 3B and 3C; Figures S2A, S2B, S2D, and S2E). Although this phenotype can result from an anchoring defect caused by a lack of Long Osk protein, this is not the case for *slimb* mutants as Long Osk is present at normal or even slightly elevated levels. Thus, this phenotype may reflect a failure to degrade Osk that is not at the posterior cortex or the production of so much Short Osk that it can no longer be efficiently anchored.

As an alternative approach to investigate where in the oocyte Slimb targets Osk for degradation, we analyzed the localization of GFP-Slimb-Δ-F-Box, which cannot rescue Slimb function but interacts with Slimb substrates and therefore reveals their distribution. GFP-Slimb-Δ-F-Box reproduces Osk localization in *slimb* mutants, forming a broad posterior crescent (Figure S2G). Furthermore, both Osk protein and GFP-Slimb-Δ-F-Box are found in the center of the *slimb* mutant oocytes that display polarity defects (Figures S2C and S2H). Osk translation is thought to be repressed until *osk* mRNA reaches the oocyte

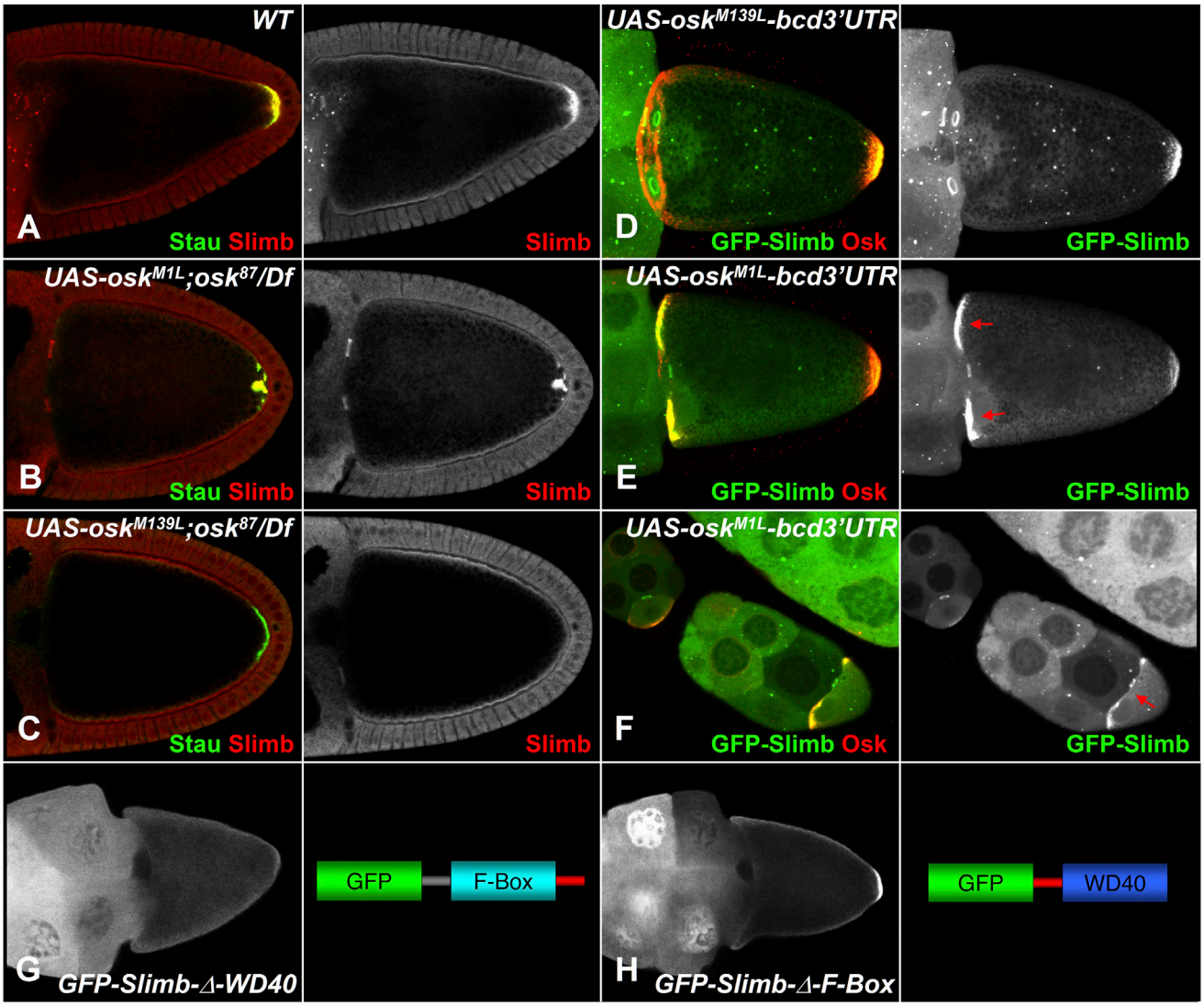

Figure 2. Slimb Localization Depends on Its Substrate Interaction Domain and Short Osk

(A–F) Slimb is recruited by Short Osk, but not Long Osk. (A–C) Egg chambers of the indicated genotypes were stained for Stau (Green) and Slimb (red). (A) Endogenous Slimb forms a posterior crescent in wild-type oocytes. (B) Slimb still colocalizes with Stau at the posterior of *UAS-osk^{M1L};osk^{A87}/Df(3R)p^{XT103}* oocytes, which only express Short Osk, although Stau and *osk* mRNA are not anchored at the posterior. (C) Slimb is not localized to the posterior of *UAS-osk^{M139L};osk^{A87}/Df(3R)p^{XT103}* oocytes that express only Long Osk. (D) GFP-Slimb (green) is not recruited to the anterior by Long Osk expressed from UAS-oskM139L-bcd3′UTR but still localizes posteriorly with endogenous Osk. (E and F) GFP-Slimb is recruited to the anterior by Short Osk expressed from *UAS-osk^{M1L}-bcd3′UTR* in stage 10A (E) and stage 7 (F) oocytes.

(G and H) Slimb's substrate interaction domain is necessary and sufficient for posterior localization. (G) GFP-Slimb-Δ-WD40 does not localize to the posterior. (H) GFP-Slimb-Δ-F-Box, which contains the substrate interaction domain, but lacks the F-Box domain, localizes to the oocyte posterior. A schematic representation of the domains is shown. (A–H) GFP-Slimb and Osk transgenes were expressed using *nanos-GAL4:VP16*.

See also Figure S1.

posterior, but this phenotype indicates that some mRNA escapes this repression and that the resulting mislocalized protein is normally targeted for degradation by Slimb. To further analyze the potential role of Slimb in removing excess Osk protein, we compared the effects of overexpressing Osk in wild-type and *slimb* oocytes. When Osk is overexpressed in wild-type oocytes, Osk forms an enlarged posterior crescent and is often found in an additional ectopic dot but is excluded from most of the oocyte cortex (Figure 3E; Zimyanin et al., 2007). By contrast, overexpression of Osk in *slimb* mutants results in its accumulation all over the oocyte cortex (Figures 3F and 3F'). Slimb therefore limits the levels of Osk protein at the posterior and also degrades mislocalized Osk, indicating that it targets Osk for degradation wherever it is made in the oocyte. We do not, however, detect any accumulation of Osk in the nurse cells in Osk-overexpressing egg chambers, suggesting that *osk* mRNA translation is fully repressed in the nurse cells or that any Osk protein is removed by an alternative degradation pathway.

The SCF^{-Slimb} ubiquitin ligase catalyzes the linkage of a polyubiquitin chain to its substrates, thereby targeting them for

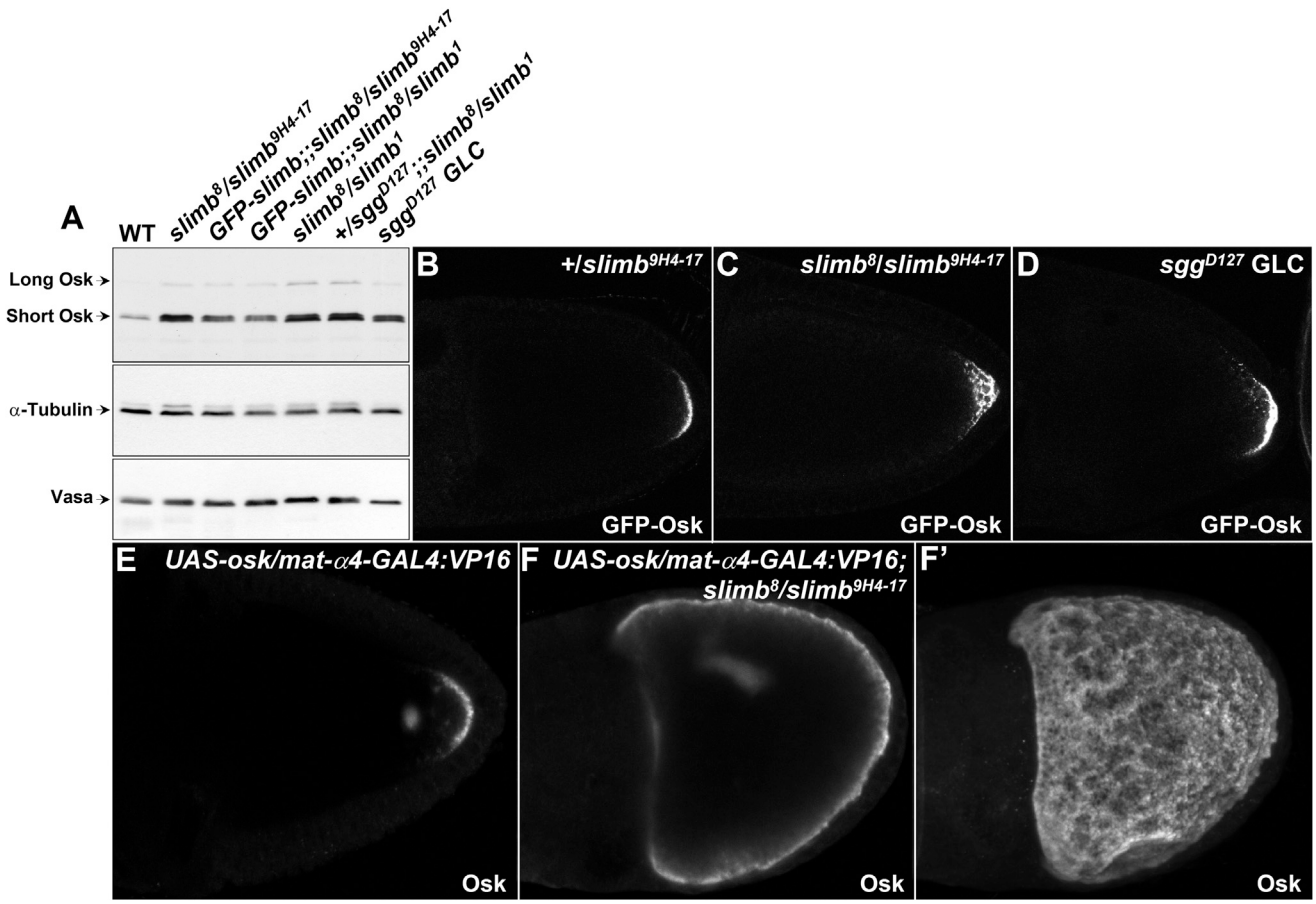

Figure 3. Slimb Regulates Osk Protein Levels

(A) Osk is stabilized in *slimb* and *sgg* mutants. Western blots of ovary extracts from the indicated genotypes were probed with α-Osk and α-tubulin/α-Vasa as loading controls. The levels of Short Osk are significantly increased in sgg^{D127} germline clones and in $slimb^{8}/slimb^{9H4-17}$ transheterozygotes that have been rescued to adulthood by hs-Slimb expression in the larva and dissected 3 to 4 days after the last period of Slimb induction. GFP-Slimb expression reduces Osk levels in *slimb* mutants (lanes 3–4).

(B–D) Osk-GFP expression in stage 9 oocytes from heterozygous control (B), $slimb^{8}/slimb^{9H4-17}$ (C), and sgg^{D127} germline clones (D).

(E) Osk localization in an oocyte in which *osk* mRNA has been overexpressed using the *mat-α4-GAL4:VP16* to drive UAS-*osk*. *osk* mRNA overexpression disrupts oocyte polarity, leading to the ectopic Osk protein in the oocyte center, but does not strongly increase Osk protein levels.

(F and F') Osk localization in a *UAS-osk/mat-α4-GAL4:VP16;slimb*^{8}*/slimb*^{9H14} oocyte. In the absence of Slimb, *osk* mRNA overexpression leads to the accumulation of Osk protein all over the oocyte cortex. (F') is a z stack projection from the oocyte shown in (F) to show the uniform cortical localization of Osk protein. See also Figure S2.

degradation by the 26S proteasome. Poly- and monoubiquitylated proteins can be detected by staining with the FK2 antibody, which does not bind free ubiquitin (Fujimuro et al., 1994). FK2 staining produces a specific signal at the posterior of most wild-type oocytes, which is particularly clear at stage 10 of oogenesis (Figure S2K). This signal is strongly reduced in *slimb* mutant oocytes and completely absent in osk^{84}/Df mutants, indicating that Slimb and Osk protein are required for the accumulation of ubiquitylated proteins at the posterior (Figures S2L and S2M). Furthermore, mild Osk overexpression driven by *nanos-GAL4:VP16* increases the posterior staining of ubiquitylated species, whereas strong overexpression driven by *mat-α4-GAL4:VP16* induces FK2 staining in a dot in the middle of the oocyte that overlaps with ectopically localized Osk (Figures S2N and S2O). Finally, the FK2 signal at the posterior of the oocyte is not due to the accumulation of ubiquitylated pole plasm components, because it persists in the vas^{PD} mutant, which abolishes pole plasm formation downstream of Osk (Figure S2P). These results are consistent with the idea that SCF^{-Slimb} polyubiquitylates Osk protein to target it for degradation.

Shaggy Kinase Localizes to the Oocyte Posterior and Regulates Osk Protein Stability

Slimb recruits the SCF complex to its substrates by recognizing a phosphorylated destruction motif. In a number of cases, such as Armadillo/β-catenin and Cubitus interruptus, the recruitment of Slimb requires phosphorylation of this motif by Shaggy (Sgg), the *Drosophila* ortholog of Glycogen synthase kinase-3 (GSK-3) (Maniatis, 1999). We therefore tested whether Sgg is also required to regulate Osk protein levels. Western blots of ovary extracts from *sgg* germline clones show elevated levels of Osk protein, and Osk-GFP accumulates to higher levels at

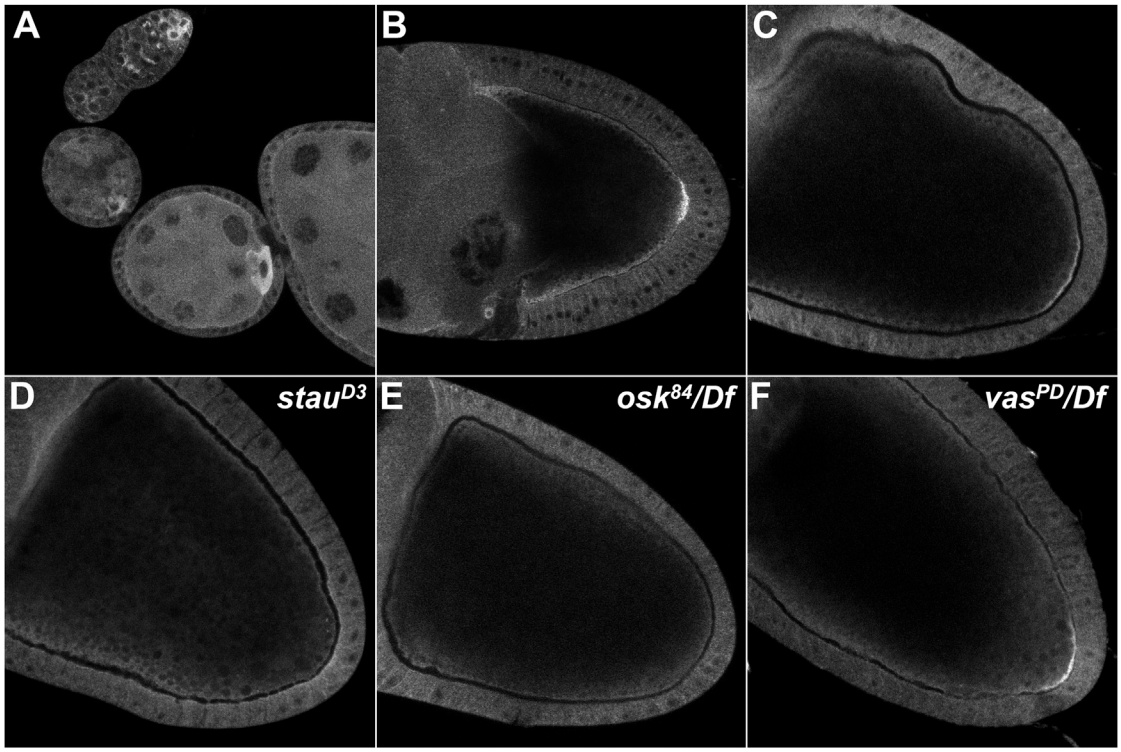

Figure 4. Shaggy Localizes to the Posterior of the Oocyte
Localization of Sgg (GSK-3) is visualized using the *sgg*$^{CPTI\text{-}000854}$ GFP protein trap line. Sgg accumulates in the oocyte from early oogenesis onward (A) and forms a crescent at the oocyte posterior from late stage 9 to stage 11 (B and C) but is absent in oocytes mutant for *stau* (D) or *osk* (E). Sgg localizes normally in *vasa* mutants (F).

the posterior of *sgg* mutant oocytes (Figures 3A and 3D). Furthermore, a GFP protein trap insertion in *sgg* that reports the localization of endogenous Sgg accumulates in the oocyte during early oogenesis and localizes in a crescent at the posterior of the oocyte at stages 9–11 (Figures 4A–4C). As this localization mirrors that of Slimb, we next examined whether it has the same requirements. The posterior localization of Sgg is disrupted in *stau* and *osk* mutants but is maintained in a strong hypomorphic *vasa* allele, *vas*^{PD} (Figures 4D–4F). Thus, like Slimb, Sgg localization requires Osk protein but is upstream of the formation of the pole plasm. This suggests that Sgg may phosphorylate Osk to target it for Slimb-mediated degradation.

Par-1 Phosphorylates Osk at Ser248, Priming It for Sgg/GSK-3 Phosphorylation on Ser244

To determine whether Sgg/GSK-3 can phosphorylate Osk directly, we performed in vitro kinase assays using recombinant rabbit GSK-3 and Osk but observed no phosphorylation of Osk. Given that Par-1 has been previously shown to phosphorylate Osk (Riechmann et al., 2002), we used Par-1 as a positive control to analyze Osk phosphorylation. We confirmed that Osk is phosphorylated by both recombinant MBP-Par-1 and GFP-Par-1 immunoprecipitated from ovaries (Figures 5A and 5B). Furthermore, no Osk phosphorylation was observed when we immunoprecipitated a kinase-dead version of GFP-Par-1, ruling out the possibility of phosphorylation by a copurifying kinase (Figure 5B). Surprisingly, Par-1 did not phosphorylate the expected region of Osk (292–606) (Riechmann et al., 2002) and instead phosphorylated a more N-terminal fragment spanning amino acids (aa) 217–294 (Figures 5A and 5C). We mapped this phosphorylation replacing each serine or threonine in this region with alanine by site-directed mutagenesis, except for Ser244 and Ser248, where the alanine substitutions were unstable in *Escherichia coli* and serine was replaced with glutamate instead. This analysis revealed that mutation of Ser248 alone was sufficient to abolish phosphorylation of this fragment, whereas none of the other mutations had any detectable effect (Figures 5D and 5E).

To test whether Par-1 phosphorylates Osk on S248 in vivo, we generated a phosphospecific antibody against Osk$^{S248\text{-}P}$. This antibody detects a crescent at the posterior of the oocyte at stage 9 that corresponds to the site of Osk localization and appears to specifically recognize phosphorylated Osk, as treating the oocytes with λ phosphatase abolishes this localized signal (Figure 5F). To confirm the specificity of the antibody, we generated oocytes expressing a nonphosphorylatable form of Osk (Osk^{S248A}; see below) in an *osk* protein null mutant background. Although Osk^{S248A} protein localizes normally to the posterior of the oocyte, it is not detected by the anti- Osk$^{S248\text{-}P}$ antibody, verifying that the antibody specifically recognizes Osk that is phosphorylated on S248 (Figure 5G). No staining for Osk$^{S248\text{-}P}$ is observed at the site of Osk localization in the middle of *par-1* mutant oocytes, indicating that this phosphorylation depends on Par-1 kinase (Figure 5F). Taken together, these results demonstrate that Par-1 phosphorylates Osk in vivo on S248.

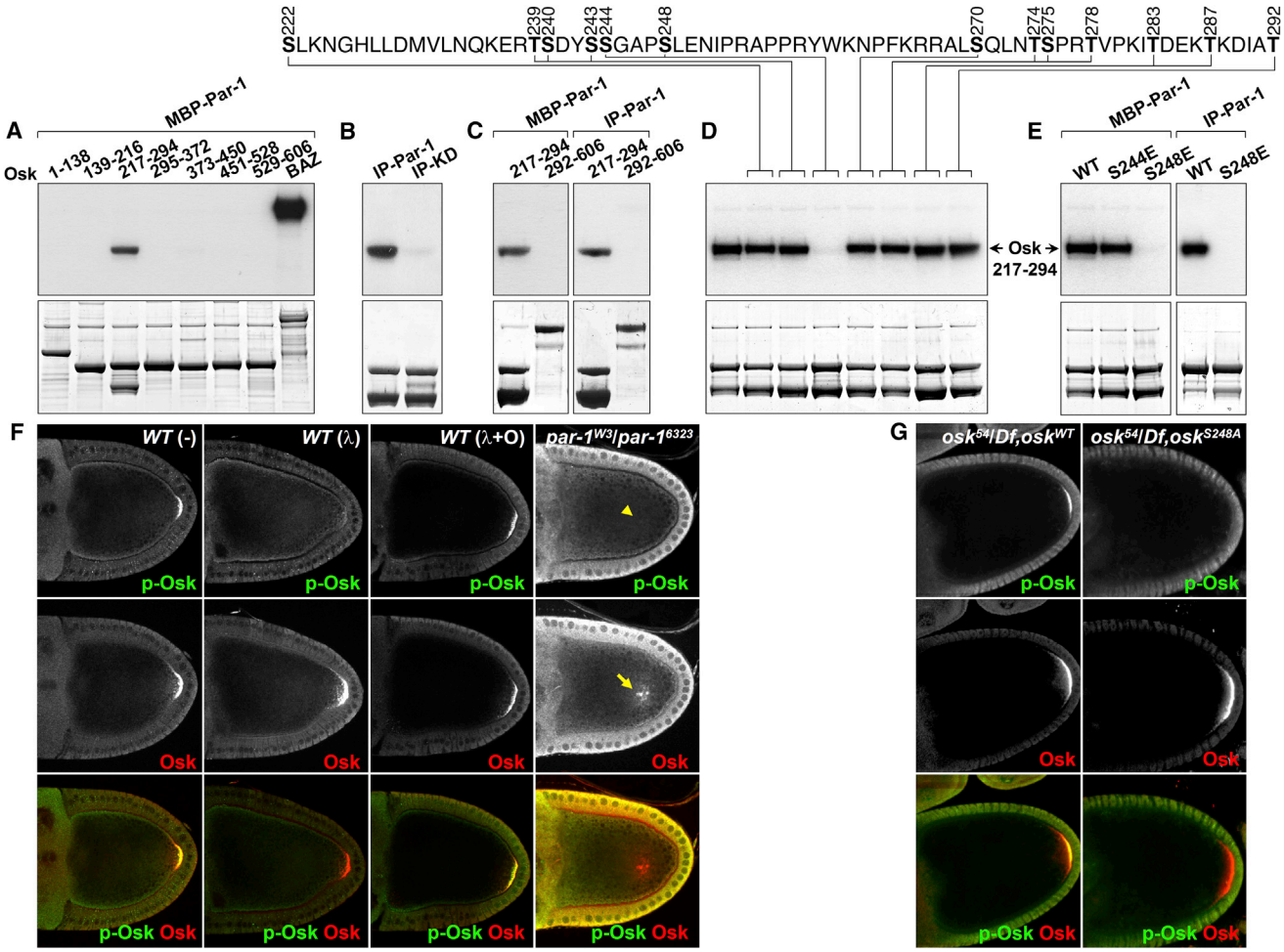

Figure 5. Par-1 Phosphorylates Osk on Serine 248

(A) In vitro kinase assay using purified recombinant MBP-Par-1 (amino acids 245–521) incubated with Osk protein fragments spanning the entire protein, expressed as MBP fusions.

(B) In vitro kinase assay using GFP-Par-1 (IP-Par-1) or GFP-Par-1 kinase dead (IP-KD) purified from ovarian extracts by immunoprecipitation with α-GFP and MBP-Osk217-294 as a substrate.

(C) In vitro kinase assays using purified MBP-Par-1 or immunoprecipitated GFP-Par-1 incubated with the MBP-Osk 217-294 and MBP-Osk292-606. Only Osk217-294 is phosphorylated, indicating that there are no Par-1 phosphorylation sites in the Osk C-terminal region.

(D) In vitro kinase assay with recombinant MBP-Par-1 and Osk217-294 containing point mutations in putative phosphorylation sites. All fragments show wild-type levels of phosphorylation, except the S444E, S248E mutant, which is not phosphorylated.

(E) In vitro kinase assays using MBP-Par-1 or IP-Par-1 incubated with Osk217-292 S244E and Osk217-292 S248E. The S248E mutation abolishes phosphorylation, identifying S248 as the Par-1 phosphorylation site. The lower panels in (A)–(E) show gels stained with Instant Blue before autoradiography to verify that each reaction contained equal amounts of substrate.

(F) Wild-type or *par-1*^{W3}/*par-1*^{6323} stage 10 egg chambers stained with an antibody that recognizes Osk phosphorylated on S248 (p-Osk, green) and anti-Osk (red). The wild-type egg chambers received no treatment (–), were treated with λ phosphatase to remove phosphate groups (λ), or were treated with λ phosphatase + Na_3VO_4, which blocks phosphatase activity (λ+O). Note that Osk is found in the middle of *par-1* mutant oocytes (arrow), but it is not detected by p-Osk (arrowhead).

(G) Stage 10 egg chambers from *osk*^{54}/*Df(3R)p*^{XT103} females carrying one copy of a wild-type genomic *osk* construct (*osk*^{WT}) or a construct in which S248 is mutated to alanine (*osk*^{S248A}) stained with α-Osk^{S248-P} or α-Osk. The phosphospecific antibody does not stain Osk^{S248A} protein, although it is highly expressed at the posterior of the oocyte, confirming the specificity of the antibody for Osk phosphorylated on S248.

The sequence surrounding the Par-1 phosphorylation site (SSGAPS) resembles the consensus site for phosphorylation by GSK-3 (T/SXXXSp/Tp), which requires a priming phosphorylation in the +4 position (Dajani et al., 2001; Fiol et al., 1987). We therefore performed in vitro kinase assays to ask whether GSK-3 could phosphorylate Osk after it had been phosphorylated by Par-1. Recombinant GSK-3 is unable to phosphorylate Osk^{WT} alone (Figure 6A, lane 2). However, when both Par-1 and GSK-3 are added to the reaction, Osk^{WT} is much more phosphorylated than by Par-1 alone (lane 3, compared to lane 1). This increase in Osk phosphorylation on adding GSK-3 is not observed with Osk^{S244E}, which is mutant for the predicted GSK-3 phosphorylation site, and this protein is phosphorylated by Par-1 and GSK-3 to the same extent as by Par-1 alone

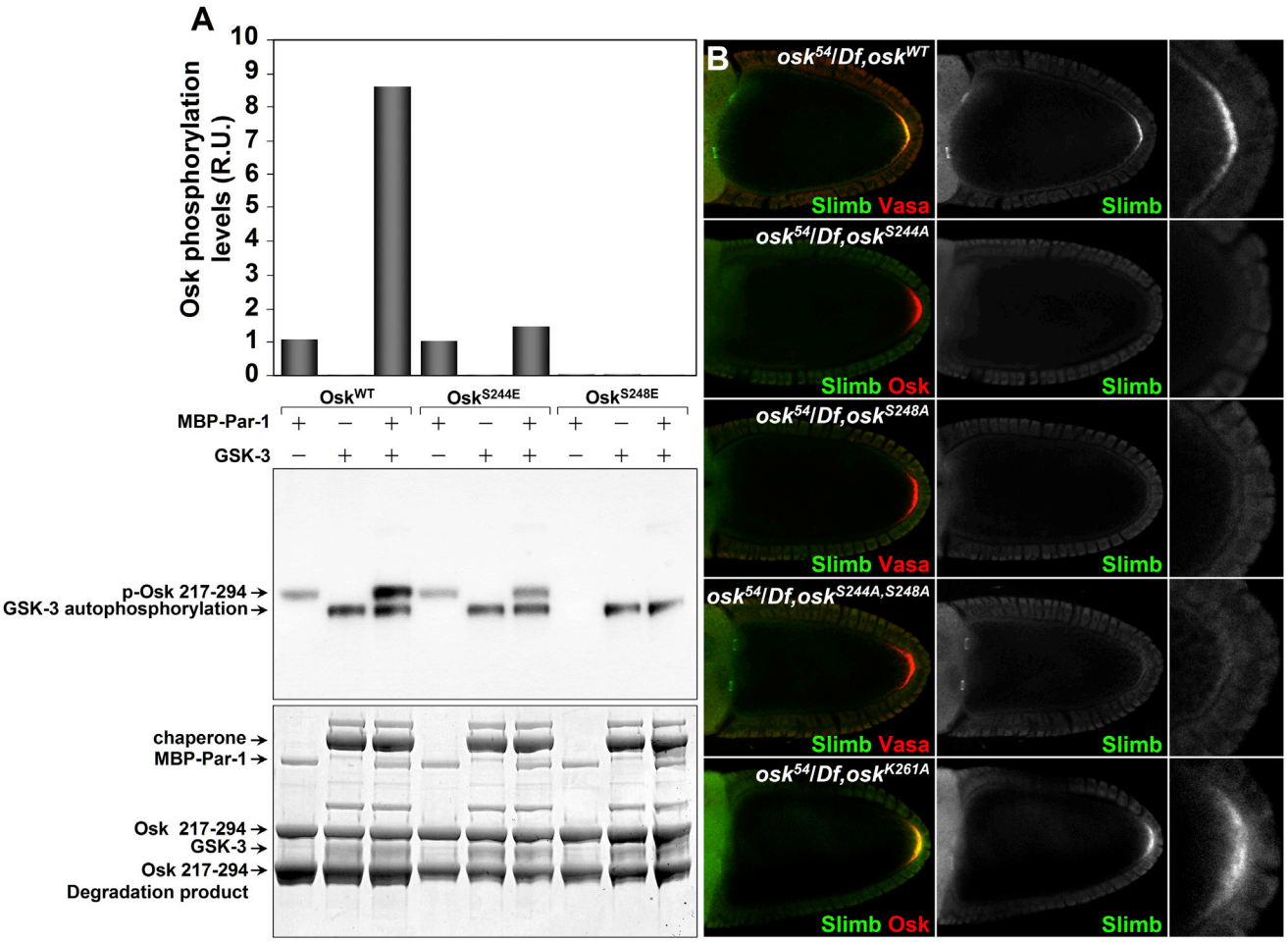

Figure 6. Par-1 Primes Osk for GSK-3 Phosphorylation and Slimb Recruitment

(A) In vitro kinase assays with MBP-Par-1 and GSK-3 in reactions containing wild-type Osk217-294 (Osk^{WT}), Osk^{S244E}, or Osk^{S248E} as substrates. MBP-Par-1 was added 25 min before the addition of GSK-3. Osk^{WT} is more highly phosphorylated when Par-1 and GSK-3 are added sequentially, but the S244 mutation blocks the enhancement upon GSK-3 addition, and the S248 mutation blocks all phosphorylation. This indicates that GSK-3 phosphorylates S244, but only if S248 is already phosphorylated.

(B) Egg chambers expressing wild-type or nonphosphorylatable forms of Osk in an Osk protein null mutant background were stained for Slimb (green) and Vasa (red) or Osk (red). Slimb is recruited to the posterior by Osk^{WT} and Osk^{K261A}, but not by Osk that cannot be phosphorylated by GSK-3 (Osk^{S244A}) or Par-1 (Osk^{S248A}), or the double mutant ($Osk^{S244A,S248A}$).

See also Movie S1.

(lane 6, compared to lanes 1 and 4). In addition, Osk^{S248E} is not phosphorylated in any of the conditions tested (lanes 7–9), demonstrating that phosphorylation of S248 by Par-1 is required for the subsequent phosphorylation of S244 by GSK-3.

Slimb Is Recruited to Doubly Phosphorylated Osk

The region of Osk that is phosphorylated by Par-1 and GSK-3 closely matches the consensus for the Slimb degron (DSpGφXSp - φ; hydrophobic, X; any amino acid), suggesting that sequential phosphorylation by these two kinases recruits Slimb to target Osk for degradation. To test this hypothesis, we mutated each or both phosphorylation sites to alanine within a full-length *osk* genomic fragment to produce nonphosphorylatable versions of Osk that are expressed from the endogenous promoter. These transgenes were integrated into the same genomic *attB* site using PhiC31 integrase-mediated recombination and crossed into an osk^{54}/Df background. Each transgene is therefore expressed at the same level and provides the only source of Osk in the oocyte. Osk^{WT} protein recruits Slimb to the oocyte posterior as expected, whereas Osk^{S244A}, Osk^{S248A}, and $Osk^{S244A,S248A}$ do not (Figure 6B). Thus, both serines are required for Slimb recruitment, consistent with the idea that the sequential phosphorylation of Osk by Par-1 and GSK-3 generates a Slimb binding site. Osk and its downstream effector Vasa are still present at the posterior in osk^{S244A}, osk^{S248A}, and $osk^{S244A,S248A}$ oocytes (Figure 6B; data not shown). However, three-dimensional reconstructions of stage 10 oocytes indicate that unphosphorylatable Osk^{S248A} is not as tightly localized as Osk^{WT} and spreads away from the posterior cortex (Movie S1).

Because the nonphosphorylatable *osk* mutants fail to recruit Slimb, one would expect Osk proteins to be stabilized in these mutants, and this is indeed the case: Osk^{S244A} (GSK-3 site

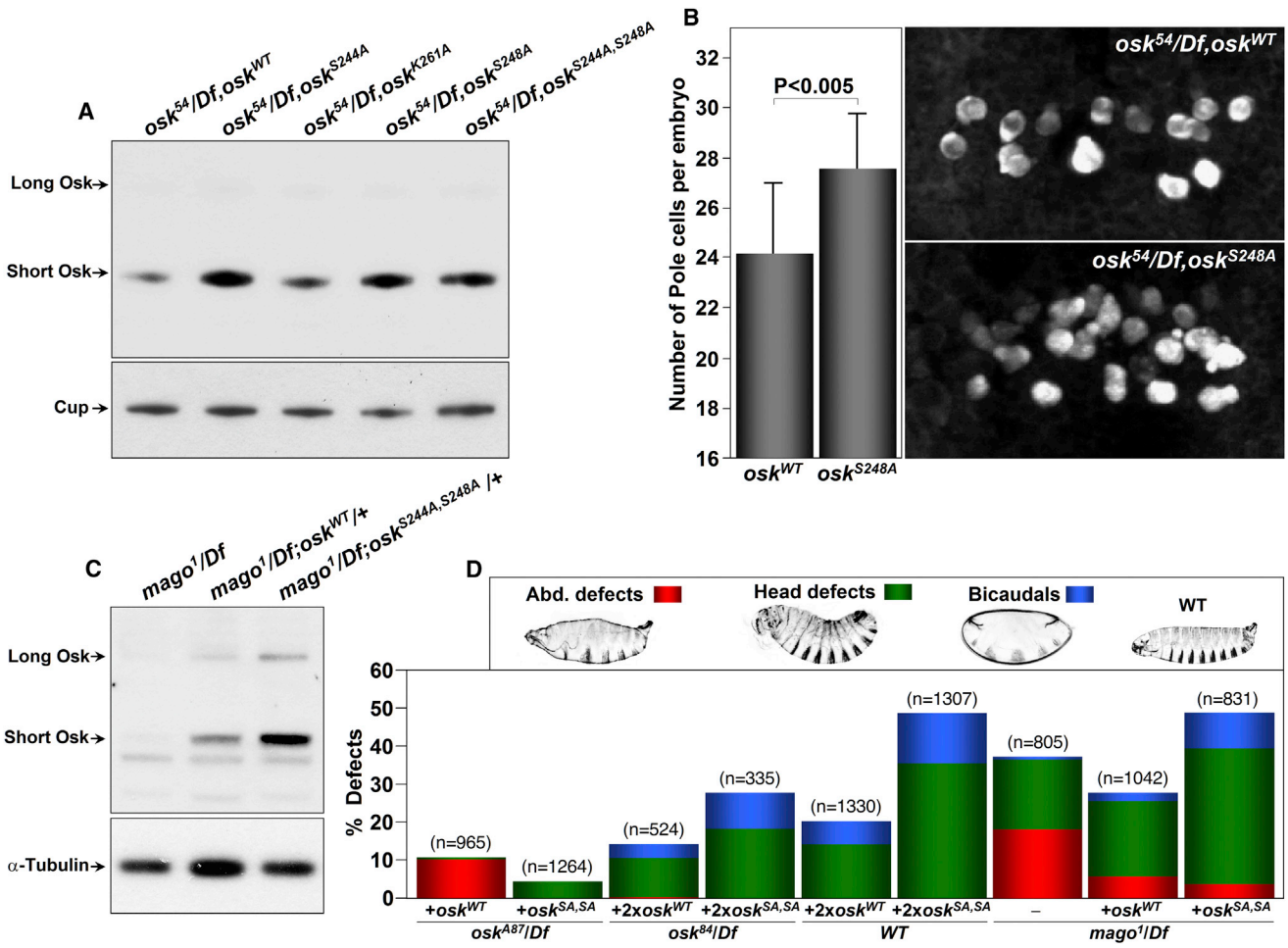

Figure 7. Nonphosphorylatable Osk Is Stabilized, Leading to Increased Numbers of Pole Cells and Patterning Defects

(A) Western blot of ovary extracts from females expressing *osk* transgenes with point mutations in the GSK-3 (Osk^{S244A}), Par-1 (Osk^{S248A}), or both phosphorylation sites ($Osk^{S244A,S248A}$) in an $osk^{54}/Df(3R)p^{XT103}$ background, probed for Osk protein. The Osk proteins with mutant phosphorylation sites accumulate to much higher levels than the wild-type protein (Osk^{WT}) expressed from the same insertion site.

(B) Expression of nonphosphorylatable Osk leads to an increase in pole cell number. The left panel shows the average number of pole cells ± SD per embryo in 12 embryos from $osk^{54}/Df(3R)p^{XT103}$, osk^{WT} mothers and $osk^{54}/Df(3R)p^{XT103}$, osk^{S248A} mothers ($p < 0.005$, Student's t test with a two-tailed distribution). The right panel shows projections of stage 11 embryos stained with Vasa to mark the pole cells.

(C) Nonphosphorylatable Osk accumulates in *mago* mutants. Western blot of ovary extracts from $mago^{1}/Df(2R)F36$ females carrying no transgene, with one copy of Osk^{WT} or with one copy of $Osk^{S244A,S248A}$ probed with α-Osk. The membrane was reprobed with α-tubulin as a loading control.

(D) Quantification of the phenotypes at 25°C of embryos derived from $osk^{A87}/Df(3R)p^{XT103}$, $osk^{84}/Df(3R)p^{XT103}$, wild-type, and $mago^{1}/Df(2R)F36$ females carrying the indicated copies of Osk^{WT} or $Osk^{S244A,S248A}$ transgenes.

mutant), Osk^{S248A} (Par-1 site mutant), and $Osk^{S244A,S248A}$ accumulate to higher levels than Osk^{WT} in ovary extracts (Figure 7A). This is consistent with a model in which the recruitment of SCF^{-Slimb} complex catalyzes the polyubiquitylation of Osk to target it for degradation by the proteosome. SCF^{-Slimb} attaches polyubiquitin chains to lysine residues, which are usually located near the phosphodegron, and Osk contains lysines in appropriate positions (K236, K261). Mutation of either K236 or K261 had, however, no effect on Osk stability, suggesting that other lysines can be used as Ubiquitin acceptors (Figure 7A; data not shown).

The nonphosphorylatable *osk* mutants provide a way of testing the in vivo significance of the regulation of Osk stability by Par-1, GSK-3, and SCF^{-Slimb} that is not possible with mutations in any of these *trans*-acting factors, which all disrupt other processes in oogenesis (Muzzopappa and Wappner, 2005; Shulman et al., 2000; Tomancak et al., 2000). Both single phosphorylation site mutant transgenes (osk^{S244A} and osk^{S248A}) and the double mutant transgene ($osk^{S244A,S248A}$) gave similar phenotypes, consistent with the fact that they all block Slimb recruitment. Because Osk nucleates the pole plasm, which contains the posterior determinant, *nanos* mRNA, and the pole cell determinants, the number of pole cells provides a sensitive readout for the level of Osk activity (Ephrussi and Lehmann, 1992; Smith et al., 1992). Embryos from mothers expressing one copy of nonphosphorylatable Osk contain an average of 28 pole cells, compared to 24 in embryos from mothers expressing one copy of Osk^{WT} ($p < 0.005$) (Figure 7B). This small but significant increase is less than one might expect from the observed increase

in Osk protein levels but may reflect the fact that much of the additional Osk in the nonphosphorylatable mutants is not tightly localized to the posterior.

We also assayed the ability of the transgenes to rescue the abdominal defects of the *osk* null mutant. One copy of osk^{WT} rescued the arrest in oogenesis of *osk* mRNA null (osk^{A87}/*Df*) flies. However, 10% of the resulting embryos were missing abdominal segments, displaying a weak posterior group phenotype (Figure 7D). By contrast, one copy of nonphosphorylatable Osk rescued abdomen formation completely but also produced a significant frequency of embryos with head defects, which are characteristic of Osk overexpression. Furthermore, 20% of the embryos laid by females with two copies of the $osk^{S244A,S248A}$ transgene in an *osk* protein null background developed head defects, and 10% were symmetric bicaudals, whereas two copies of the wild-type transgene in the same background produced a much lower frequency of anterior defects. The effect of mutating the two phosphorylated serines in Osk is also apparent when the transgenes are expressed in the presence of wild-type *osk*. Nonphosphorylatable Osk produces three times as many embryos with head defects as Osk^{WT}, with 19 % bicaudal embryos. Thus, the nonphosphorylatable mutants frequently disrupt anterior development in both *osk* mutant and wild-type backgrounds, demonstrating that Slimb-dependent degradation of Osk is important for normal anterior-posterior axis formation.

The head defects produced by nonphosphorylatable Osk expression can be caused by too much Osk at the posterior but are most commonly due to mislocalized anterior Osk, which recruits ectopic Nanos to repress the translation of *bicoid* mRNA (Ephrussi and Lehmann, 1992; Wharton and Struhl, 1991). This phenotype and the recruitment of Slimb to the anterior of oocytes expressing *osk-bcd3′*UTR raise the possibility that degradation plays a key role in removing mislocalized Osk protein. To test this hypothesis directly, we crossed one copy of osk^{WT} or $osk^{S244A,S248A}$ into *mago nashi* (*mago*) mutant females, in which most *osk* mRNA is mislocalized to the anterior of the oocyte (Boswell et al., 1991). The addition of one extra copy of osk^{WT} results in a small increase in the levels of Osk protein and partially rescues the abdominal phenotype of the resulting embryos (Figures 7C and 7D). The levels of Osk are, however, much higher in the presence of one copy of $osk^{S244A,S248A}$, and almost none of the embryos develop abdominal defects. Instead, nearly half the embryos have head defects, with 19% showing the more severe, symmetric bicaudal phenotype (Figures 7C and 7D). Taken together, these results indicate that Par-1/GSK-3/Slimb-dependent degradation plays a key role in repressing Osk accumulation at the anterior of the oocyte to prevent ectopic Nanos from disrupting head development.

DISCUSSION

The results presented here reveal a mode of Osk regulation that appears to play two important roles in development. First, by reducing the amount of Osk protein that accumulates at the correct site at the posterior of the oocyte, SCF^{-Slimb}-dependent degradation limits the amount of pole plasm produced and thereby restricts the number of pole cells (the primordial germ cells) that form in the early embryo. This activity therefore regulates the balance between the germline and the soma, a key decision point in development that is under strong selective pressure (Strome and Lehmann, 2007). Perhaps more importantly, Osk degradation also serves to remove Osk from inappropriate regions of the oocyte. *osk* mRNA is translationally repressed until it is localized, and this is thought to be the main mechanism that restricts Osk protein to the oocyte posterior (Kim-Ha et al., 1995; Markussen et al., 1995; Rongo et al., 1995). However, even unlocalized *osk* mRNA sediments in the polysomal fraction in sucrose gradients, suggesting that this mRNA is translated (Braat et al., 2004; Chekulaeva et al., 2006). Because even small amounts of ectopic Osk protein are sufficient to disrupt head development, the translation of unlocalized *osk* mRNA even at low levels means that there must be a mechanism to get rid of this ectopic protein (Braat et al., 2004). Our results demonstrate that unlocalized *osk* mRNA is indeed translated, as nonphosphorylatable Osk protein accumulates in *mago* oocytes, in which *osk* mRNA transport to the posterior is impaired. Furthermore, SCF^{-Slimb}-dependent degradation provides the mechanism that removes this mislocalized Osk protein, as the translation of Osk^{WT} from the mRNA at the anterior of *mago* mutants only rarely disrupts head development, whereas Osk that cannot recruit Slimb causes a significant frequency of bicaudal embryos. Thus, the translational repression of unlocalized *osk* mRNA is leaky and is not sufficient on its own to restrict Osk protein to the posterior, and Slimb-dependent degradation provides an essential backup mechanism to dispose of small amounts of mislocalized Osk.

Slimb is recruited to Osk by a typical phosphodegron that must undergo two sequential phosphorylations to be recognized, much like other well-characterized Slimb/β-TRCP substrates, such as Armadillo/β-catenin, Cubitus Interruptus, and IκB (Fuchs et al., 2004; Smelkinson et al., 2007). Osk is targeted for degradation by Par-1 phosphorylation, which primes it for a second phosphorylation four amino acids downstream by GSK-3, to generate a strong Slimb binding site that recruits the SCF^{-Slimb} complex. Our data show that only the pole plasm inducing isoform Short Osk is able to recruit Slimb. As Long Osk also contains the Slimb binding site, the folding of its additional N-terminal extension may block phosphorylation or the interaction with Slimb.

The role of Par-1 in Osk degradation is surprising, given a previous report that Par-1 phosphorylation stabilizes Osk (Riechmann et al., 2002). The reasons for this discrepancy are unclear, but there are several differences between the two analyses that may account for this contradiction. First, the in vitro phosphorylation experiments performed by Riechmann et al. (2002) used a truncated version of Osk (aa 292–606) that lacks serine 248, which is the only site that was strongly phosphorylated by Par-1 in our analysis of the entire protein. Second, they assayed the stability of truncated in vitro translated Osk in *Drosophila* protein extracts and *Xenopus* oocytes, which may not reflect the regulation that occurs in the normal context of the *Drosophila* oocyte. Although we cannot rule out the possibility that Par-1 phosphorylates other, lower efficiency sites in Osk, our data strongly suggest that the major effect of Par-1 phosphorylation on Osk protein is to target it for polyubiquitylation and degradation by the proteasome. The phosphospecific antibody against Osk^{S248-P} confirms that serine 248 is phosphorylated in vivo, and mutation of this site to alanine stabilizes the protein.

Furthermore, when *osk* mRNA is overexpressed in *par-1* mutants, the levels of Osk protein are hugely increased compared to *osk* mRNA overexpression in a wild-type background, and ectopic protein accumulates all over the oocyte (Zimyanin et al., 2007).

Par-1 plays at least two positive roles in Osk regulation. First, the recruitment of Par-1 to the posterior cortex of the oocyte in response to the polarizing signal from the posterior follicle cells induces the repolarization of the oocyte microtubule cytoskeleton that directs *osk* mRNA localization to the posterior pole (Doerflinger et al., 2006, 2010; Shulman et al., 2000; Tomancak et al., 2000). Because *osk* mRNA is released from translational repression at the posterior, its localization enhances the synthesis of Osk protein. Second, Osk protein recruits a distinct population of Par-1 to its site of accumulation, and this reinforces the polarity of the microtubule cytoskeleton to increase the localization of *osk* mRNA (Zimyanin et al., 2007). The results presented here show that Par-1 also negatively regulates Osk by targeting it for degradation. Because Osk protein is degraded by the Par-1/GSK-3/Slimb pathway wherever it is made within the oocyte and not just at the posterior pole, Osk is presumably phosphorylated by the second population of Par-1 that is recruited by Osk protein itself.

It seems paradoxical that Par-1 participates in both positive and negative feedback loops to regulate Osk levels, but one reason why this might be important is suggested by the fact that Par-1 positively regulates *osk* mRNA localization but negatively regulates the accumulation of Osk protein. *osk* mRNA can only be transported by kinesin to the posterior of the oocyte during stages 9–10A of oogenesis, when the microtubule cytoskeleton is polarized with the plus ends extending toward the posterior pole, as the microtubules are rearranged by the fast cytoplasmic streaming that begins at stage 10B (Dahlgaard et al., 2007; Manseau et al., 1996; Parton et al., 2011; Zimyanin et al., 2008). By contrast, Osk protein only accumulates to high levels during stages 13–14 of oogenesis, coincident with the decline of Slimb localization to the posterior (Snee et al., 2007). Thus, Par-1 seems to induce a temporal delay between the localization of *osk* mRNA and the accumulation of Short Osk protein. During stages 9–10A, Par-1 acts to polarize the microtubule cytoskeleton to promote the efficient localization of *osk* mRNA, while preventing the excessive accumulation of Short Osk. The mRNA is then stably anchored at the posterior by Long Osk, which does not recruit Slimb. At the end of oogenesis, the Par-1/GSK-3/Slimb pathway appears to be less active, and high levels of Short Osk accumulate so that the pole plasm can assemble just before it is needed to induce pole cell formation in the fertilized egg. These results highlight the central role that Par-1 plays in defining the posterior and regulating the assembly of the pole plasm, both in space and time.

EXPERIMENTAL PROCEDURES

Drosophila Strains and Genetics

Drosophila strains and genetics are described in detail in the Supplemental Experimental Procedures.

sgg^{D127} germline clones (GLC) were produced using the dominant female sterile technique (Chou and Perrimon, 1996). Although *slimb* mutations are recessive lethal, *slimb* mutant adults can be obtained by inducing Slimb expression under the control of a heat shock promoter in first-instar larvae until the end of pupariation (Grima et al., 2002). Transheterozygous $slimb^{8}$/$slimb^{9H4-17}$ mutants were analyzed 3 to 4 days after the last period of hs-Slimb induction.

In Vitro Kinase Assays

In vitro kinase assays were performed as previously described (Benton et al., 2002). Recombinant rabbit GSK-3 was purchased from New England BioLabs and used at 1 μg per reaction. The full protocol is described in the Supplemental Experimental Procedures.

Immunological Methods

An antibody against phosphoserine 248 of Osk was raised in rabbits by injection of the phosphorylated peptide SDYSSGAP[pS]LENIPRAP and subsequent immunodepletion with the unmodified peptide SDYSSGAPSLENIPRAP and affinity purification with the phosphorylated peptide (21st Century Biochemicals). Immunofluorescence (IF) and western blotting were performed in accordance with standard protocols using antibodies described in the Supplemental Experimental Procedures. Actin was visualized with rhodamine-conjugated phalloidin (Invitrogen).

SUPPLEMENTAL INFORMATION

Supplemental Information includes Supplemental Experimental Procedures, two figures, and one movie and can be found with this article online at http://dx.doi.org/10.1016/j.devcel.2013.06.011.

ACKNOWLEDGMENTS

We would like to thank A. Ephrussi, D. Kalderon, P. Lasko, P. Macdonald, A. Nakamura, G. Rogers, F. Royer, and the Bloomington Stock Center for providing fly stocks and antibodies. This work was supported by a Wellcome Trust Principal Research Fellowship (049818 and 080007 to D.StJ.) and core support from the Wellcome Trust (092096) and Cancer Research UK (A14492). E.M. was supported by the Portuguese Foundation for Science and Technology (FCT), A.V.R. was supported by a FEBS Long-Term Fellowship, and V.T. was supported by an EU Marie Curie Fellowship (236621).

Received: January 22, 2013
Revised: May 24, 2013
Accepted: June 11, 2013
Published: August 12, 2013

REFERENCES

Benton, R., Palacios, I.M., and St Johnston, D. (2002). *Drosophila* 14-3-3/PAR-5 is an essential mediator of PAR-1 function in axis formation. Dev. Cell *3*, 659–671.

Boswell, R.E., Prout, M.E., and Steichen, J.C. (1991). Mutations in a newly identified *Drosophila melanogaster* gene, *mago nashi*, disrupt germ cell formation and result in the formation of mirror-image symmetrical double abdomen embryos. Development *113*, 373–384.

Braat, A.K., Yan, N., Arn, E., Harrison, D., and Macdonald, P.M. (2004). Localization-dependent oskar protein accumulation; control after the initiation of translation. Dev. Cell *7*, 125–131.

Breitwieser, W., Markussen, F.H., Horstmann, H., and Ephrussi, A. (1996). Oskar protein interaction with Vasa represents an essential step in polar granule assembly. Genes Dev. *10*, 2179–2188.

Cardozo, T., and Pagano, M. (2004). The SCF ubiquitin ligase: insights into a molecular machine. Nat. Rev. Mol. Cell Biol. *5*, 739–751.

Chekulaeva, M., Hentze, M.W., and Ephrussi, A. (2006). Bruno acts as a dual repressor of *oskar* translation, promoting mRNA oligomerization and formation of silencing particles. Cell *124*, 521–533.

Chou, T.B., and Perrimon, N. (1996). The autosomal FLP-DFS technique for generating germline mosaics in *Drosophila melanogaster*. Genetics *144*, 1673–1679.

Clark, I., Giniger, E., Ruohola-Baker, H., Jan, L.Y., and Jan, Y.N. (1994). Transient posterior localization of a kinesin fusion protein reflects anteroposterior polarity of the *Drosophila* oocyte. Curr. Biol. *4*, 289–300.

Dahlgaard, K., Raposo, A.A., Niccoli, T., and St Johnston, D. (2007). Capu and Spire assemble a cytoplasmic actin mesh that maintains microtubule organization in the *Drosophila* oocyte. Dev. Cell *13*, 539–553.

Dajani, R., Fraser, E., Roe, S.M., Young, N., Good, V., Dale, T.C., and Pearl, L.H. (2001). Crystal structure of glycogen synthase kinase 3 beta: structural basis for phosphate-primed substrate specificity and autoinhibition. Cell *105*, 721–732.

Doerflinger, H., Benton, R., Torres, I.L., Zwart, M.F., and St Johnston, D. (2006). *Drosophila* anterior-posterior polarity requires actin-dependent PAR-1 recruitment to the oocyte posterior. Curr. Biol. *16*, 1090–1095.

Doerflinger, H., Vogt, N., Torres, I.L., Mirouse, V., Koch, I., Nüsslein-Volhard, C., and St Johnston, D. (2010). Bazooka is required for polarisation of the *Drosophila* anterior-posterior axis. Development *137*, 1765–1773.

Ephrussi, A., and Lehmann, R. (1992). Induction of germ cell formation by *oskar*. Nature *358*, 387–392.

Ephrussi, A., Dickinson, L.K., and Lehmann, R. (1991). Oskar organizes the germ plasm and directs localization of the posterior determinant nanos. Cell *66*, 37–50.

Fiol, C.J., Mahrenholz, A.M., Wang, Y., Roeske, R.W., and Roach, P.J. (1987). Formation of protein kinase recognition sites by covalent modification of the substrate. Molecular mechanism for the synergistic action of casein kinase II and glycogen synthase kinase 3. J. Biol. Chem. *262*, 14042–14048.

Fuchs, S.Y., Spiegelman, V.S., and Kumar, K.G. (2004). The many faces of beta-TrCP E3 ubiquitin ligases: reflections in the magic mirror of cancer. Oncogene *23*, 2028–2036.

Fujimuro, M., Sawada, H., and Yokosawa, H. (1994). Production and characterization of monoclonal antibodies specific to multi-ubiquitin chains of polyubiquitinated proteins. FEBS Lett. *349*, 173–180.

González-Reyes, A., and St Johnston, D. (1994). Role of oocyte position in establishment of anterior-posterior polarity in *Drosophila*. Science *266*, 639–642.

Grima, B., Lamouroux, A., Chélot, E., Papin, C., Limbourg-Bouchon, B., and Rouyer, F. (2002). The F-box protein slimb controls the levels of clock proteins period and timeless. Nature *420*, 178–182.

Ikeda, S., Kishida, S., Yamamoto, H., Murai, H., Koyama, S., and Kikuchi, A. (1998). Axin, a negative regulator of the Wnt signaling pathway, forms a complex with GSK-3beta and beta-catenin and promotes GSK-3beta-dependent phosphorylation of beta-catenin. EMBO J. *17*, 1371–1384.

Jaramillo, A.M., Weil, T.T., Goodhouse, J., Gavis, E.R., and Schupbach, T. (2008). The dynamics of fluorescently labeled endogenous *gurken* mRNA in *Drosophila*. J. Cell Sci. *121*, 887–894.

Jia, J., Amanai, K., Wang, G., Tang, J., Wang, B., and Jiang, J. (2002). Shaggy/GSK3 antagonizes Hedgehog signalling by regulating Cubitus interruptus. Nature *416*, 548–552.

Kim-Ha, J., Smith, J.L., and Macdonald, P.M. (1991). *oskar* mRNA is localized to the posterior pole of the *Drosophila* oocyte. Cell *66*, 23–35.

Kim-Ha, J., Kerr, K., and Macdonald, P.M. (1995). Translational regulation of *oskar* mRNA by bruno, an ovarian RNA-binding protein, is essential. Cell *81*, 403–412.

Kugler, J.M., and Lasko, P. (2009). Localization, anchoring and translational control of *oskar, gurken*, *bicoid* and *nanos* mRNA during *Drosophila* oogenesis. Fly (Austin) *3*, 15–28.

Liang, L., Diehl-Jones, W., and Lasko, P. (1994). Localization of vasa protein to the *Drosophila* pole plasm is independent of its RNA-binding and helicase activities. Development *120*, 1201–1211.

Maniatis, T. (1999). A ubiquitin ligase complex essential for the NF-kappaB, Wnt/Wingless, and Hedgehog signaling pathways. Genes Dev. *13*, 505–510.

Manseau, L., Calley, J., and Phan, H. (1996). Profilin is required for posterior patterning of the *Drosophila* oocyte. Development *122*, 2109–2116.

Markussen, F.H., Michon, A.M., Breitwieser, W., and Ephrussi, A. (1995). Translational control of *oskar* generates short OSK, the isoform that induces pole plasma assembly. Development *121*, 3723–3732.

Martin, S.G., Leclerc, V., Smith-Litière, K., and St Johnston, D. (2003). The identification of novel genes required for *Drosophila* anteroposterior axis formation in a germline clone screen using GFP-Staufen. Development *130*, 4201–4215.

Muzzopappa, M., and Wappner, P. (2005). Multiple roles of the F-box protein Slimb in *Drosophila* egg chamber development. Development *132*, 2561–2571.

Parton, R.M., Hamilton, R.S., Ball, G., Yang, L., Cullen, C.F., Lu, W., Ohkura, H., and Davis, I. (2011). A PAR-1-dependent orientation gradient of dynamic microtubules directs posterior cargo transport in the *Drosophila* oocyte. J. Cell Biol. *194*, 121–135.

Price, M.A., and Kalderon, D. (2002). Proteolysis of the Hedgehog signaling effector Cubitus interruptus requires phosphorylation by Glycogen Synthase Kinase 3 and Casein Kinase 1. Cell *108*, 823–835.

Riechmann, V., Gutierrez, G.J., Filardo, P., Nebreda, A.R., and Ephrussi, A. (2002). Par-1 regulates stability of the posterior determinant Oskar by phosphorylation. Nat. Cell Biol. *4*, 337–342.

Rongo, C., Gavis, E.R., and Lehmann, R. (1995). Localization of *oskar* RNA regulates *oskar* translation and requires Oskar protein. Development *121*, 2737–2746.

Roth, S., Neuman-Silberberg, F.S., Barcelo, G., and Schüpbach, T. (1995). *cornichon* and the EGF receptor signaling process are necessary for both anterior-posterior and dorsal-ventral pattern formation in *Drosophila*. Cell *81*, 967–978.

Shulman, J.M., Benton, R., and St Johnston, D. (2000). The *Drosophila* homolog of C. elegans PAR-1 organizes the oocyte cytoskeleton and directs *oskar* mRNA localization to the posterior pole. Cell *101*, 377–388.

Smelkinson, M.G., and Kalderon, D. (2006). Processing of the *Drosophila* hedgehog signaling effector Ci-155 to the repressor Ci-75 is mediated by direct binding to the SCF component Slimb. Curr. Biol. *16*, 110–116.

Smelkinson, M.G., Zhou, Q., and Kalderon, D. (2007). Regulation of Ci-SCFSlimb binding, Ci proteolysis, and hedgehog pathway activity by Ci phosphorylation. Dev. Cell *13*, 481–495.

Smith, J.L., Wilson, J.E., and Macdonald, P.M. (1992). Overexpression of *oskar* directs ectopic activation of nanos and presumptive pole cell formation in *Drosophila* embryos. Cell *70*, 849–859.

Snee, M.J., Harrison, D., Yan, N., and Macdonald, P.M. (2007). A late phase of Oskar accumulation is crucial for posterior patterning of the *Drosophila* embryo, and is blocked by ectopic expression of Bruno. Differentiation *75*, 246–255.

St Johnston, D., and Ahringer, J. (2010). Cell polarity in eggs and epithelia: parallels and diversity. Cell *141*, 757–774.

St Johnston, D., Beuchle, D., and Nüsslein-Volhard, C. (1991). Staufen, a gene required to localize maternal RNAs in the *Drosophila* egg. Cell *66*, 51–63.

Strome, S., and Lehmann, R. (2007). Germ versus soma decisions: lessons from flies and worms. Science *316*, 392–393.

Tanaka, T., and Nakamura, A. (2008). The endocytic pathway acts downstream of Oskar in *Drosophila* germ plasm assembly. Development *135*, 1107–1117.

Tomancak, P., Piano, F., Riechmann, V., Gunsalus, K.C., Kemphues, K.J., and Ephrussi, A. (2000). A *Drosophila melanogaster* homologue of *Caenorhabditis elegans par-1* acts at an early step in embryonic-axis formation. Nat. Cell Biol. *2*, 458–460.

Vanzo, N.F., and Ephrussi, A. (2002). Oskar anchoring restricts pole plasm formation to the posterior of the *Drosophila* oocyte. Development *129*, 3705–3714.

Weil, T.T., Forrest, K.M., and Gavis, E.R. (2006). Localization of *bicoid* mRNA in late oocytes is maintained by continual active transport. Dev. Cell *11*, 251–262.

Wharton, R.P., and Struhl, G. (1991). RNA regulatory elements mediate control of *Drosophila* body pattern by the posterior morphogen *nanos*. Cell *67*, 955–967.

Zimyanin, V., Lowe, N., and St Johnston, D. (2007). An oskar-dependent positive feedback loop maintains the polarity of the *Drosophila* oocyte. Curr. Biol. *17*, 353–359.

Zimyanin, V.L., Belaya, K., Pecreaux, J., Gilchrist, M.J., Clark, A., Davis, I., and St Johnston, D. (2008). In vivo imaging of *oskar* mRNA transport reveals the mechanism of posterior localization. Cell *134*, 843–853.